REPORT 1018

A THEORETICAL ANALYSIS OF THE EFFECT OF TIME LAG IN AN AUTOMATIC STABILIZATION SYSTEM ON THE LATERAL OSCILLATORY STABILITY OF AN AIRPLANE [1]

By LEONARD STERNFIELD and ORDWAY B. GATES, Jr.

SUMMARY

A method is presented for determining the effect of time lag in an automatic stabilization system on the lateral oscillatory stability of an airplane. The method is based on an analytical-graphical procedure. The critical time lag of the airplane-autopilot system is readily determined from the frequency-response analysis.

The method is applied to a typical present-day airplane equipped with an automatic pilot sensitive to yawing acceleration and geared to the rudder so that rudder control is applied in proportion to the yawing acceleration. The results calculated for this airplane-autopilot system by this method are compared with the airplane motions calculated by a step-by-step procedure.

INTRODUCTION

Recent calculations and flight tests of several airplanes designed for operation in the transonic speed range have indicated unsatisfactory damping of the lateral oscillation. The results presented in reference 1 show that the oscillatory stability can be improved by the use of an automatic pilot. The calculations of reference 1, however, were made on the assumption of an idealized control system without lag. Reference 2 points out that lag of the type in which the amount of control applied at a given instant is assumed to be proportional to a deviation which existed at a fixed time previous to the given instant can be represented mathematically by use of the lag operator $e^{-\tau_s D_b}$, where τ_s is nondimensional time lag based on the span and D_b is the differential operator. Lag of this type is generally referred to as time lag. Reference 2 suggests that for purposes of calculation the lag operator may be approximated by three terms of the Taylor's series for $e^{-\tau_s D_b}$. This approximation was used in some recent calculations (reference 3) and the results were found to be erroneous and misleading. The purpose of this report is to present a satisfactory method for determining the effect of time lag on the lateral oscillatory stability based on the exact expression of the lag operator rather than any approximation. Some recent analyses on the same problem, unknown to the authors at the time this problem was being analyzed, are presented in references 4 and 5.

SYMBOLS AND COEFFICIENTS

ϕ	angle of roll, radians
ψ	angle of yaw, radians
β	angle of sideslip, radians (v/V)
r	yawing angular velocity, radians per second $(d\psi/dt)$
$\dot{r}$	yawing angular acceleration, radians per second per second $(d^2\psi/dt^2)$
p	rolling angular velocity, radians per second $(d\phi/dt)$
v	sideslip velocity along lateral axis, feet per second
V	airspeed, feet per second
ρ	mass density of air, slugs per cubic foot
q	dynamic pressure, pounds per square foot $\left(\frac{1}{2}\rho V^2\right)$
b	wing span, feet
S	wing area, square feet
W	weight of airplane, pounds
m	mass of airplane, slugs (W/g)
g	acceleration due to gravity, feet per second per second
μ_b	relative-density factor $(m/\rho Sb)$
η	inclination of principal longitudinal axis of airplane with respect to flight path, positive when principal axis is above flight path at nose, degrees
γ	angle of flight path to horizontal axis, positive in a climb, degrees
k_{x_0}	radius of gyration in roll about principal longitudinal axis, feet
k_{z_0}	radius of gyration in yaw about principal vertical axis, feet
K_{x_0}	nondimensional radius of gyration in roll about principal longitudinal axis (k_{x_0}/b)
K_{z_0}	nondimensional radius of gyration in yaw about principal vertical axis (k_{z_0}/b)
K_X	nondimensional radius of gyration in roll about longitudinal stability axis $\left(\sqrt{K_{x_0}^2\cos^2\eta+K_{z_0}^2\sin^2\eta}\right)$

[1] Supersedes NACA TN 2005, "A Theoretical Analysis of the Effect of Time Lag in an Automatic Stabilization System on the Lateral Oscillatory Stability of an Airplane" by Leonard Sternfield and Ordway B. Gates, Jr., 1950.

K_Z nondimensional radius of gyration in yaw about vertical stability axis $\left(\sqrt{K_{Z_0}^2 \cos^2 \eta + K_{X_0}^2 \sin^2 \eta}\right)$

K_{XZ} nondimensional product-of-inertia parameter $((K_{Z_0}^2 - K_{X_0}^2) \sin \eta \cos \eta)$

C_L trim lift coefficient $\left(\frac{W \cos \gamma}{qS}\right)$

C_l rolling-moment coefficient $\left(\frac{\text{Rolling moment}}{qSb}\right)$

C_N yawing-moment coefficient $\left(\frac{\text{Yawing moment}}{qSb}\right)$

C_Y lateral-force coefficient $\left(\frac{\text{Lateral force}}{qS}\right)$

$C_{l_\beta} = \frac{\partial C_l}{\partial \beta}$

$C_{n_\beta} = \frac{\partial C_n}{\partial \beta}$

$C_{Y_\beta} = \frac{\partial C_Y}{\partial \beta}$

$C_{n_r} = \frac{\partial C_n}{\partial \frac{rb}{2V}}$

$C_{n_p} = \frac{\partial C_n}{\partial \frac{pb}{2V}}$

$C_{l_p} = \frac{\partial C_l}{\partial \frac{pb}{2V}}$

$C_{Y_p} = \frac{\partial C_Y}{\partial \frac{pb}{2V}}$

$C_{Y_r} = \frac{\partial C_Y}{\partial \frac{rb}{2V}}$

$C_{l_r} = \frac{\partial C_l}{\partial \frac{rb}{2V}}$

$C_{n_{\delta_r}} = \frac{\partial C_n}{\partial \delta_r}$

t time, seconds

s_b nondimensional time parameter based on span (Vt/b)

D_b differential operator $\left(\frac{d}{ds_b}\right)$

P period of oscillation, seconds

$T_{1/2}$ time for amplitude of oscillation to damp to one-half its original value

δ_r deflection of control, radians

a real part of complex root of characteristic stability equation

ω angular frequency, radians per second

$\omega_s = \frac{b}{V}\omega$

$\lambda = a + i\omega_s$

τ time lag between signal for control and its actual motion, seconds

$\tau_s = \frac{V}{b}\tau$

$(\tau_s)_c$ critical time lag

K_A maximum amplitude of acceleration in yaw produced by control deflection of unit amplitude $\left(\left|\frac{\ddot{\psi}}{\delta_r}\right|_{airplane}\right)$

$(K_A)_s = \frac{b^2}{V^2} K_A$

k amplitude of control-surface oscillation produced by autopilot in response to oscillation of airplane acceleration $\left(\left|\frac{\delta_r}{\ddot{\psi}}\right|_{autopilot}\right)$

$k_s = \frac{V^2}{b^2} k$

$K_C = \frac{1}{k}$

$(K_C)_s = \frac{1}{k_s}$

θ phase angle, radians

θ_A phase angle of lag of δ_r behind $\ddot{\psi}$ when oscillating control surface forces airplane to oscillate, radians

θ_C phase angle obtained from frequency response of autopilot

ANALYSIS

The investigation of the effect of time lag on the lateral oscillation may be conveniently divided into two parts: (a) determination of the smallest time lag which would result in a neutrally stable oscillation, referred to as critical time lag, and (b) the effect of a given time lag on the lateral oscillatory stability. It is important to know some of the results of the analysis obtained in part (a) in order to facilitate the analysis presented in part (b). Part (a) is based on the frequency-response method of analysis (references 6 and 7). This method affords a relatively simple means of determining the critical time lag of an automatic stabilization system and thereby of establishing the range of time lags for which the airplane motion is stable. Part (b) treats the solution of a transcendental equation by means of an analytical-graphical procedure. The analysis is presented for an airplane equipped with an automatic pilot sensitive to yawing acceleration and geared to the rudder so that rudder control is applied in proportion to the yawing acceleration, as suggested in reference 3. A similar analysis is applicable, however, to any automatic stabilization system with time lag.

The equations of motion used are expressed in terms of the nondimensional time parameter based on the span of the airplane $s_b = \frac{Vt}{b}$, but the results of the calculations obtained in terms of s_b have been converted from the nondimensional time s_b to time t in seconds. Thus the discussion of the results and the figures included in the report are given in terms of t.

DETERMINATION OF CRITICAL TIME LAG

The critical time lag of a system is defined as the time lag that results in a neutrally stable or steady-state oscillation. The motion of the control δ_r and the airplane acceleration $\ddot{\psi}$ when a critical time lag exists are shown in figure 1. This

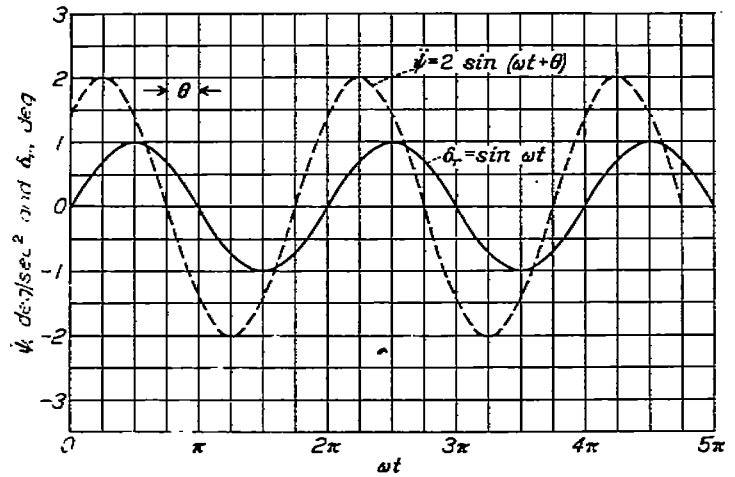

FIGURE 1.—The relationship between the airplane acceleration and the control motion for the case of critical time lag. $\theta=\omega\Delta t$; $\Delta t=\tau=\frac{\theta}{\omega}$.

figure indicates that the relationship between the time lag τ and the phase angle θ between the motion of the control and the airplane acceleration can be expressed as $\tau=\frac{\theta}{\omega}$. Since τ can be expressed as a function of θ, the frequency-response method can be utilized to determine the critical time lag for a combined airplane-autopilot system. This method requires that the frequency-response curves be calculated for the airplane and autopilot separately and the results analyzed to ascertain the conditions for neutral oscillatory stability of the airplane-autopilot system.

Frequency-response curves for airplane.—The frequency-response curves for the airplane are obtained from the calculation of the steady-state motion of the airplane in response to a sinusoidal forcing function of unit amplitude (see reference 8). Thus if

$$\delta_r=\sin\ \omega_s s_b$$

the acceleration of the airplane is

$$D_b^2\psi=(K_A)_s\sin\ (\omega_s s_b+\theta_A)$$

The values of $(K_A)_s$, known as the amplitude ratio, and θ_A are obtained over the desired range of angular frequencies by substituting $i\omega_s$ for D_b in the expression for $D_b^2\psi/\delta_r$ which is derived from the lateral equations of motion. The nondimensional lateral equations of motion, referred to stability axes, for a given control deflection are

$$\left.\begin{aligned}
&\left(2\mu_b K_X^2 D_b^2-\tfrac{1}{2}C_{l_p}D_b\right)\phi+\left(2\mu_b K_{XZ}D_b^2-\tfrac{1}{2}C_{l_r}D_b\right)\psi-C_{l_\beta}\beta=0\\
&\left(2\mu_b K_{XZ}D_b^2-\tfrac{1}{2}C_{n_p}D_b\right)\phi+\left(2\mu_b K_Z^2 D_b^2-\tfrac{1}{2}C_{n_r}D_b\right)\psi-C_{n_\beta}\beta=C_{n_{\delta_r}}\delta_r\\
&\left(-\tfrac{1}{2}C_{Y_p}D_b-C_L\right)\phi+\left(2\mu_b D_b-\tfrac{1}{2}C_{Y_r}D_b-C_L\tan\gamma\right)\psi+(2\mu_b D_b-C_{Y_\beta})\beta=0
\end{aligned}\right\}\quad(1)$$

The derivatives $C_{l_{\delta_r}}=\frac{\partial C_l}{\partial\delta_r}$ and $C_{Y_{\delta_r}}=\frac{\partial C_Y}{\partial\delta_r}$ are usually very small and therefore have been neglected in equations (1).

Hence,

$$\frac{D_b^2\psi}{\delta_r}=\frac{D_b^2\begin{vmatrix}2\mu_b K_X^2 D_b^2-\frac{1}{2}C_{l_p}D_b & 0 & -C_{l_\beta}\\ 2\mu_b K_{XZ}D_b^2-\frac{1}{2}C_{n_p}D_b & C_{n_{\delta_r}} & -C_{n_\beta}\\ -\frac{1}{2}C_{Y_p}D_b-C_L & 0 & 2\mu_b D_b-C_{Y_\beta}\end{vmatrix}}{\begin{vmatrix}2\mu_b K_X^2 D_b^2-\frac{1}{2}C_{l_p}D_b & 2\mu_b K_{XZ}D_b^2-\frac{1}{2}C_{l_r}D_b & -C_{l_\beta}\\ 2\mu_b K_{XZ}D_b^2-\frac{1}{2}C_{n_p}D_b & 2\mu_b K_Z^2 D_b^2-\frac{1}{2}C_{n_r}D_b & -C_{n_\beta}\\ -\frac{1}{2}C_{Y_p}D_b-C_L & \left(2\mu_b-\frac{1}{2}C_{Y_r}\right)D_b-C_L\tan\gamma & 2\mu_b D_b-C_{Y_\beta}\end{vmatrix}}\quad(2)$$

After the numerator and denominator are expanded by the method of determinants, the expression for $D_b^2\psi/\delta_r$ results in the ratio of two polynomials in D_b. The substitution of $i\omega_s$ for D_b in equation (2) gives a complex number $A+iB$ which may be expressed as $(K_A)_s e^{i\theta_A}$. The amplitude ratio $(K_A)_s$, which is equal to $K_A\frac{b^2}{V^2}$, can be determined from the relation $(K_A)_s=\sqrt{A^2+B^2}$. The phase angle θ_A can be determined from the relation $\theta_A=\tan^{-1}\frac{B}{A}$.

Frequency response of autopilot.—The frequency response of the autopilot is obtained from the equation for the control motion with time lag taken into account

$$\delta_r = k_s D_b^2 \psi (s_b - \tau_s) \tag{3a}$$

where the term $D_b^2\psi(s_b-\tau_s)$ signifies the fact that the amount of control applied at a given instant is proportional to the acceleration at a fixed time τ_s previous to the given instant. This time-lag effect can be expressed by the so-called lag operator $e^{-\tau_s D_b}$. Thus equation (3a) becomes

$$\delta_r = k_s D_b^2 \psi e^{-\tau_s D_b} \tag{3b}$$

Solving equation (3b) for $D_b^2\psi/\delta_r$ gives

$$\frac{D_b^2\psi}{\delta_r} = \frac{1}{k_s} e^{\tau_s D_b} = (K_C)_s e^{\tau_s D_b} \tag{4}$$

where

$$(K_C)_s = \frac{b^2}{V^2} K_C = \frac{b^2}{V^2}\left|\frac{\ddot{\psi}}{\delta_r}\right|_{autopilot}$$

Substituting $i\omega_s$ for D_b in equation (4) results in an amplitude ratio $(K_C)_s = \frac{1}{k_s}$, which is independent of frequency, and a phase angle $\theta_C = \tau_s\omega_s$.

Conditions for stability.—The necessary and sufficient conditions for any one of the oscillatory modes to be neutrally stable are that, at a particular frequency, the phase angles and amplitude ratios of the airplane and autopilot must be equal—that is, $\theta_A = \theta_C$ and $(K_A)_s = (K_C)_s$. Even though these conditions are satisfied, the resultant motion of the airplane which is composed of all the individual modes of motion may be unstable since, as is pointed out subsequently, an additional unstable oscillatory mode may be present. In general, the condition which must be satisfied in order that all the oscillatory modes be stable is that, at each angular frequency where $\theta_A = \theta_C$, the ratio $\frac{(K_A)_s}{(K_C)_s}$ must be less than 1 at that frequency. The mathematical proof of this statement is given in reference 9.

Illustrative example.—The foregoing method is applied to a typical present-day high-speed airplane having the characteristics presented in table I. The value of the control-gearing ratio k is arbitrarily assumed to be 0.0427. (This value of $k=0.0427$ corresponds to a rudder deflection of 1° for a yawing acceleration of 23.4°/sec/sec.) The amplitude-ratio and phase-angle curves for the airplane, plotted as a function of angular frequency ω, where $\omega = \omega_s \frac{V}{b}$, are presented as solid-line curves in figures 2 (a) and 2 (b), respectively. As the frequency increases to infinity, K_A approaches a value of 15.98 and θ_A approaches π. The dashed line in figure 2 (a), which is independent of frequency, is the amplitude ratio of the autopilot K_C. The phase-angle curves of the autopilot are straight lines with slopes equal to τ, where $\tau = \frac{b}{V}\tau_s$, and are shown as dashed lines in figure 2 (b) for several values of τ. Since the phase angle remains between the range of 0 to 2π, $\theta_C = \tau\omega$ continues to repeat itself whenever $\tau\omega \geqq 2\pi$. To take account of this fact, θ_C is plotted as a series of parallel lines for each value of τ. Figure 2 (a) indicates that $K_A = K_C$ at $\omega=3.8$ and $\omega=8.5$. The corresponding values of τ where $\theta_A = \theta_C$ at $\omega=3.8$ and $\omega=8.5$ are $\tau=1.63$ and $\tau=0.38$, respectively. One of the oscillatory modes of motion is thus neutrally stable when $\tau=1.63$ and $\tau=0.38$. However, as mentioned previously, the motion of the airplane is neutrally stable only if all other oscillatory modes present are stable. This condition is satisfied for $\tau=0.38$, since for each value of ω where $\theta_A = \theta_C$ the ratio $\frac{K_A}{K_C} < 1$. When $\tau=1.63$, one of the oscillatory modes is neutrally stable but the system is unstable, because at $\omega=6$, $\theta_A = \theta_C$ but $\frac{K_A}{K_C} > 1$. An analysis indicates that for values of $K_C < 15.98$, which is the limiting value of K_A, the system will be unstable for any infinitesimal time lag. The reason for the instability is that, for any infinitesimal time lag, the value of θ_A is equal to θ_C at some high frequency where it can be shown that $\frac{K_A}{K_C} > 1$ since at the very high frequencies

$$\frac{K_A}{K_C} = \frac{(K_A)_{\omega\to\infty} + \Delta K_A}{(K_A)_{\omega\to\infty} - \Delta K_C}$$

where ΔK_A and ΔK_C are small incremental values.

TABLE I.—STABILITY DERIVATIVES AND MASS CHARACTERISTICS OF A TYPICAL PRESENT-DAY AIRPLANE

W/S, lb/ft²	65
S, ft²	130
b, ft	28
ρ, slugs/ft³	0.00089
V, ft/sec	797
γ, deg	0
C_L	0.23
μ_b	80.7
K_X^2	0.00967
K_Z^2	0.0513
K_{XZ}	−0.00145
η, deg	−2.0
C_{l_p}, per radian	−0.40
C_{l_r}, per radian	0.08
C_{n_p}, per radian	−0.0155
C_{n_r}, per radian	−0.40
C_{Y_p}, per radian	0
C_{Y_r}, per radian	0
C_{Y_β}, per radian	−1.0
C_{n_β}, per radian	0.25
C_{l_β}, per radian	−0.126
$C_{n_{\delta_r}}$, per radian	−0.103

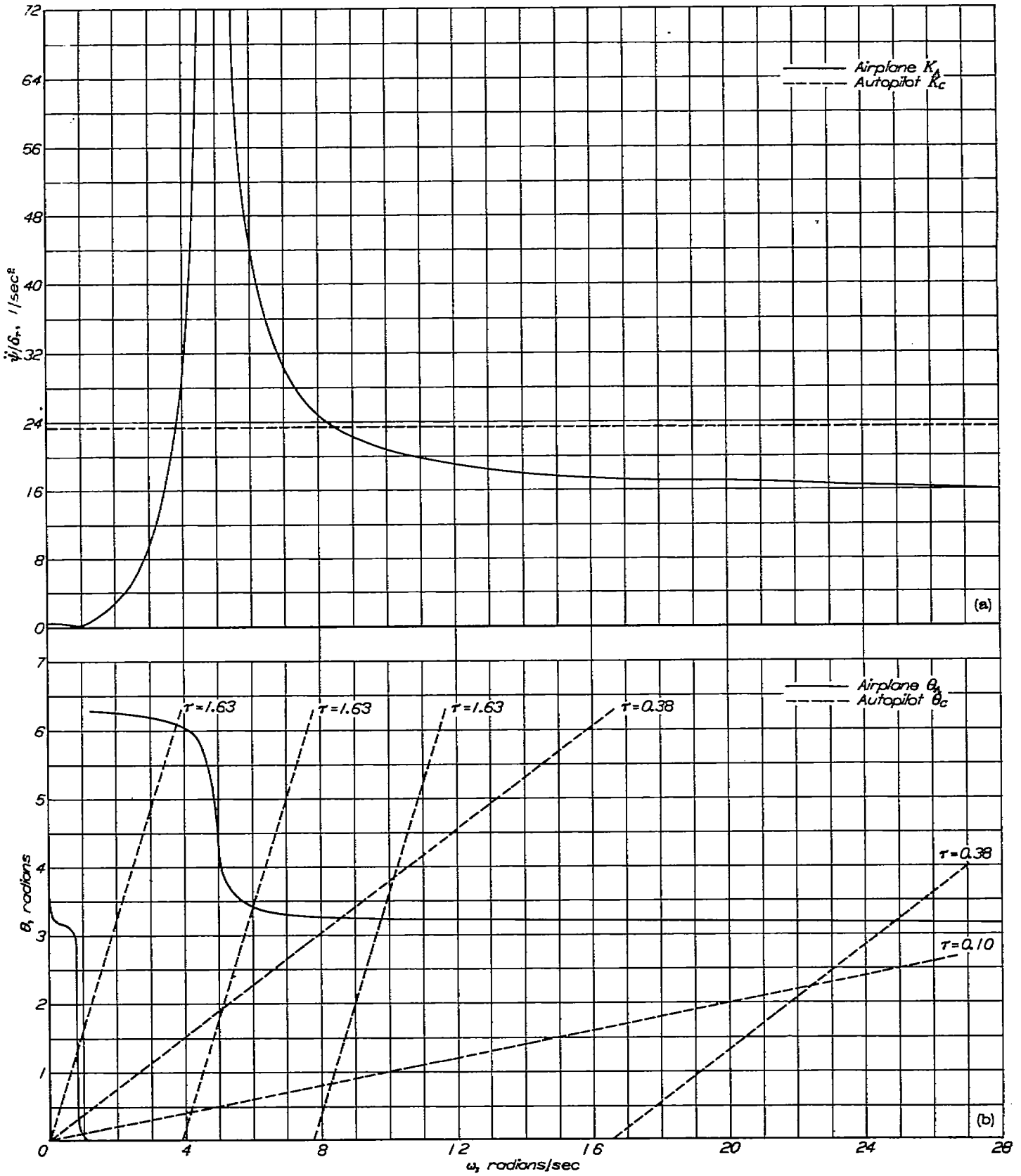

(a) Amplitude ratio.
(b) Phase angle.

FIGURE 2.—Frequency-response curves of the typical present-day airplane and the assumed autopilot.

In order to verify the results predicted by the preceding analysis, motions of the airplane were calculated subsequent to an initial disturbance of 5° in sideslip. The calculations involved a step-by-step procedure based on the Kutta 3/8 method (reference 10). The results of these calculations for $\tau=0.38$ and $\tau=1.63$ are presented in figures 3 and 4, respectively. The solid-line curve in figure 3 was obtained by using a time increment of 0.095 and the motion is seen to be slightly unstable, whereas neutral stability is predicted by frequency-response analysis for $\tau=0.38$. An additional calculation was made by using a time increment of 0.0475, represented by the dashed-line curve in figure 3, and although the motion was still slightly unstable, the trend indicated by reducing the time increment was such as to make the oscillation more nearly neutrally stable. The airplane motion for $\tau=1.63$ is presented in figure 4 and, as was predicted, the motion is unstable. A neutrally stable oscillation was also predicted for this value of time lag but it is apparent from figure 4 that the unstable mode influences the airplane motion more than the neutrally stable mode.

EFFECT OF TIME LAG ON LATERAL OSCILLATORY STABILITY

Derivation of equations.—The nondimensional equations of motion, referred to the stability axes, which include the effect of an autopilot applying rudder control in proportion to the yawing acceleration at time $s_b-\tau_s$, are obtained by combining equation (3b) with equations (1). When $\phi_0 e^{\lambda s_b}$ is substituted for ϕ, $\psi_0 e^{\lambda s_b}$ for ψ, and $\beta_0 e^{\lambda s_b}$ for β in the resultant equation written in determinant form, λ must be a root of the characteristic stability equation

$$A\lambda^4+B\lambda^3+C\lambda^2+D\lambda+E+k_s e^{-\tau_s\lambda}(A'\lambda^4+B'\lambda^3+C'\lambda^2+D'\lambda)=0 \tag{5}$$

where A, B, C, D, E, A', B', C', and D' are functions of the mass and aerodynamic parameters of the airplane. The

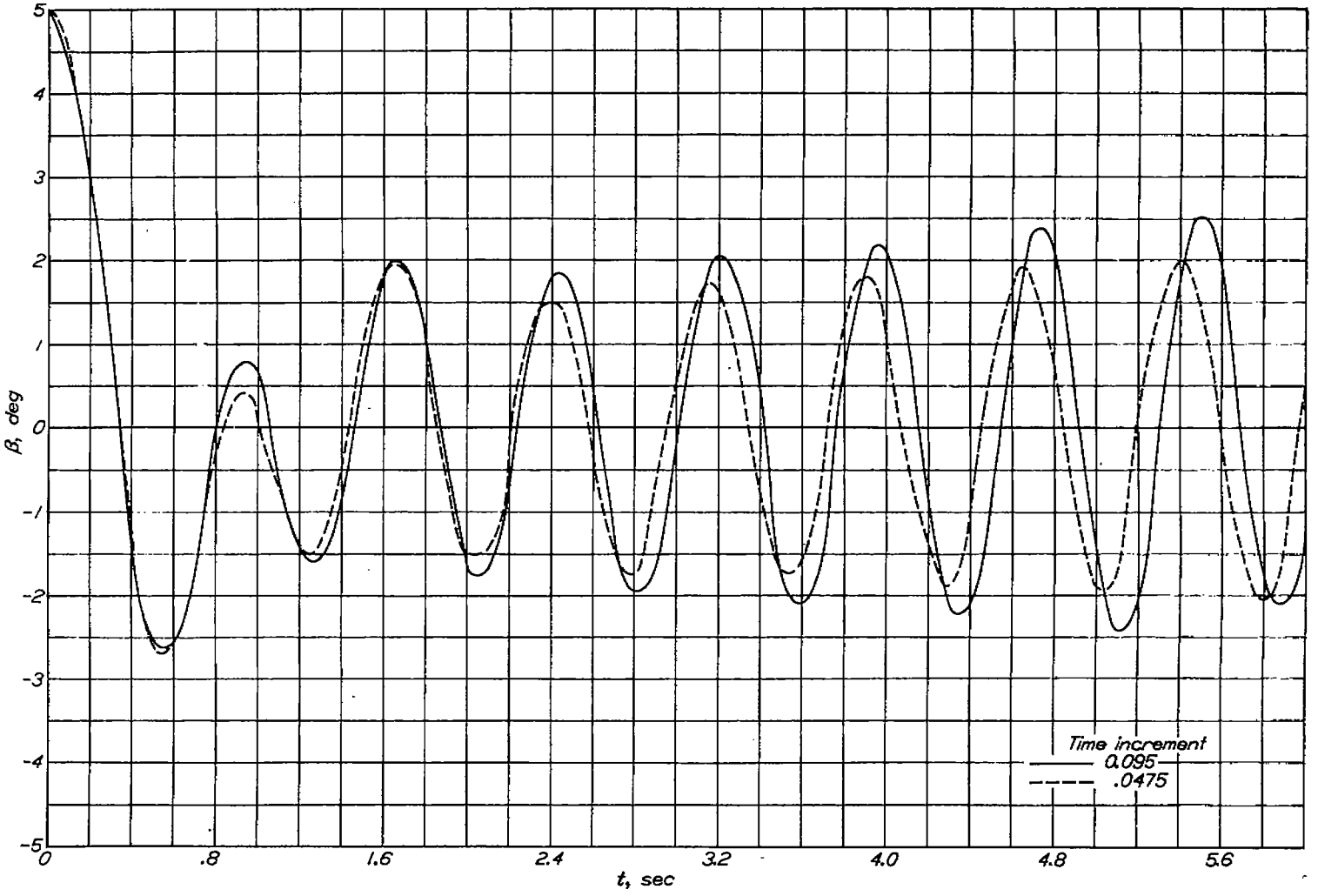

FIGURE 3.—Effect of $\tau=0.38$ on the motion of the airplane.

expressions for A, B, C, D, and E are given in reference 1 and

$$A'=-4\mu_b{}^2K_X{}^2C_{n_{\dot{\beta}_r}}$$

$$B'=(2\mu_bK_X{}^2C_{Y_\beta}+\mu_bC_{l_p})C_{n_{\dot{\beta}_r}}$$

$$C'=\left(-\frac{1}{2}C_{l_p}C_{Y_\beta}+\frac{1}{2}C_{Y_p}C_{l_\beta}\right)C_{n_{\dot{\beta}_r}}$$

$$D'=C_LC_{l_\beta}C_{n_{\dot{\beta}_r}}$$

The damping and period of the lateral oscillation in seconds are given by the expressions

$$\left.\begin{aligned}T_{\frac{1}{2}}&=\frac{-0.693}{a}\frac{b}{V}\\ P&=\frac{2\pi}{\omega_s}\frac{b}{V}\end{aligned}\right\}\qquad(6)$$

where a and ω_s are the real and imaginary parts of a complex root of equation (5).

Determination of roots of transcendental equation.—The characteristic stability equation of this system (equation (5)) is seen to be a transcendental equation because a constant time lag τ_s in the automatic stabilization system is represented by the so-called lag operator $e^{-\tau_s D_b}$. It is apparent that the complex roots of such an equation cannot be determined by conventional methods. A method of obtaining the complex roots of this transcendental equation for a particular value of τ_s is therefore presented.

If $a+i\omega_s$ is substituted for λ in equation (5) and the real and imaginary quantities are separated, two equations in a and ω_s result:

$$e^{-\tau_s a}=F_1(a,\omega_s)\qquad(7a)$$

$$e^{-\tau_s a}=F_2(a,\omega_s)\qquad(7b)$$

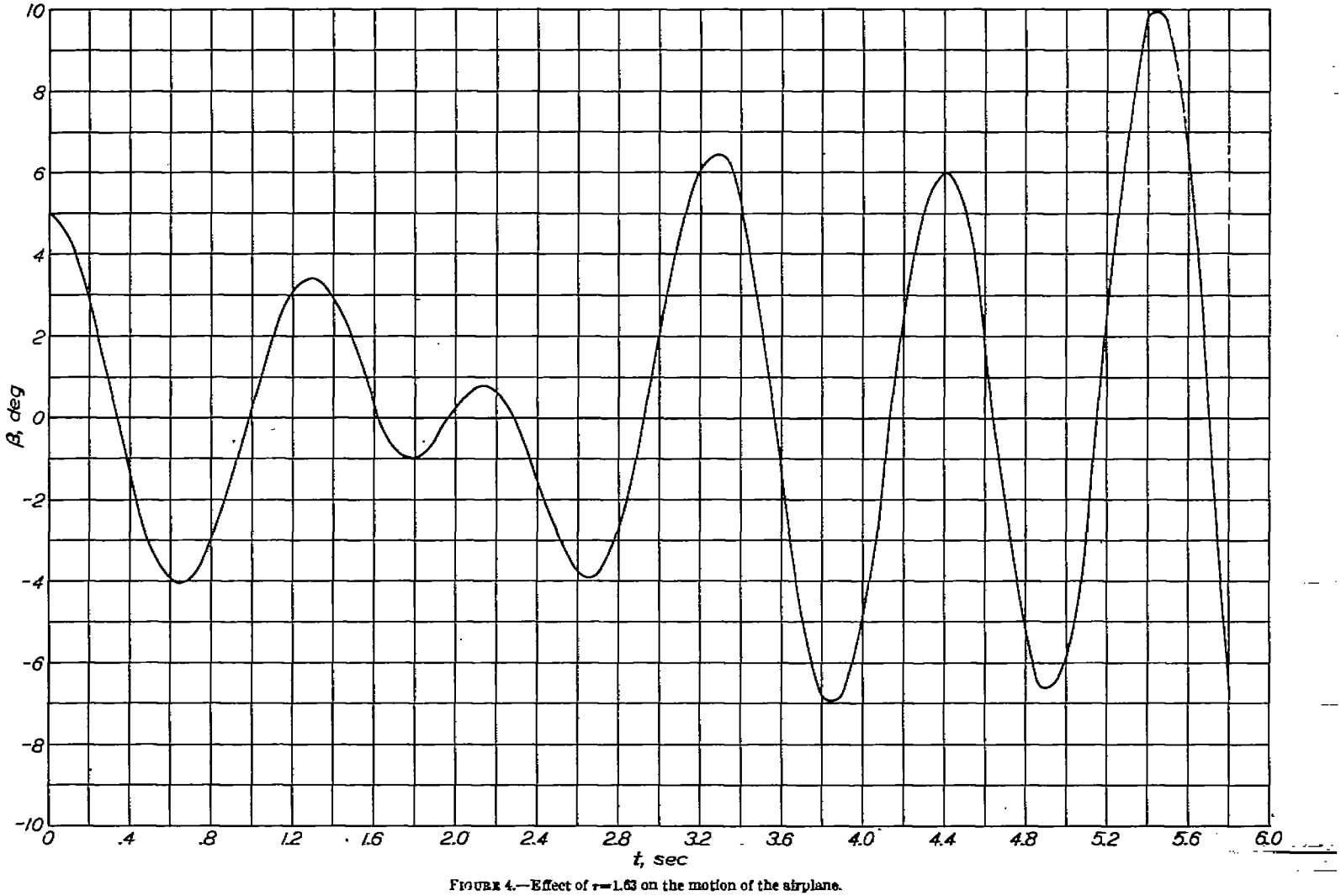

FIGURE 4.—Effect of τ=1.63 on the motion of the airplane.

A simultaneous solution of equations (7a) and (7b) gives the desired values of a and ω_s which satisfy equation (5). The method used to solve equations (7a) and (7b) simultaneously is basically a graphical procedure. For a series of values of ω_s, the right-hand sides of equations (7a) and (7b) are plotted against a as illustrated in figure 5. The solid lines and dashed lines correspond to the functions $F_1(a,\omega_s)$ and $F_2(a,\omega_s)$, respectively. The variation of $e^{-\tau_s a}$ with a is also plotted in figure 5. The exact values of a and ω_s for which $F_1(a,\omega_s)=F_2(a,\omega_s)=e^{-\tau_s a}$ are determined from a cross plot of the results of figure 5 as shown in figure 6. In this figure, with a as the abscissa and ω_s as the ordinate, are plotted the values of a and ω_s which correspond to the intersection of the $e^{-\tau_s a}$ curve with the functions $F_1(a,\omega_s)$ and $F_2(a,\omega_s)$. The solid curve in figure 6 thus satisfies the equation $e^{-\tau_s a}=F_1(a,\omega_s)$ and the dashed curve satisfies the equation $e^{-\tau_s a}=F_2(a,\omega_s)$. The values of a and ω_s at the intersection of these two curves therefore determine a root of the characteristic stability equation (equation (5)). The period and damping of the lateral oscillation are determined from equations (6) by using this root.

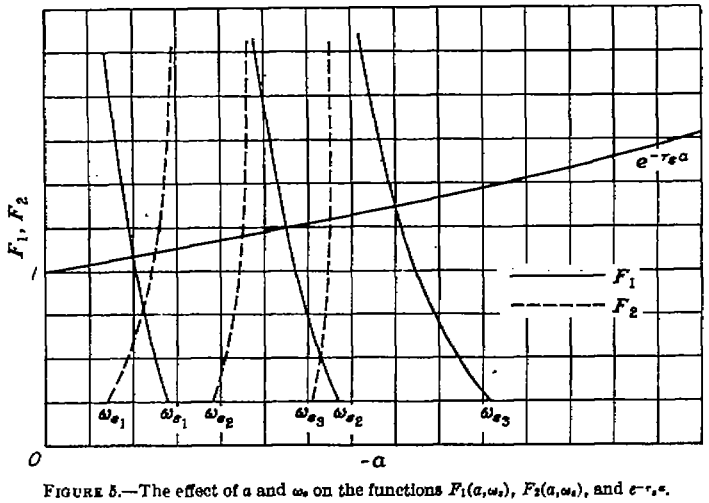

FIGURE 5.—The effect of a and ω_s on the functions $F_1(a,\omega_s)$, $F_2(a,\omega_s)$, and $e^{-\tau_s a}$.

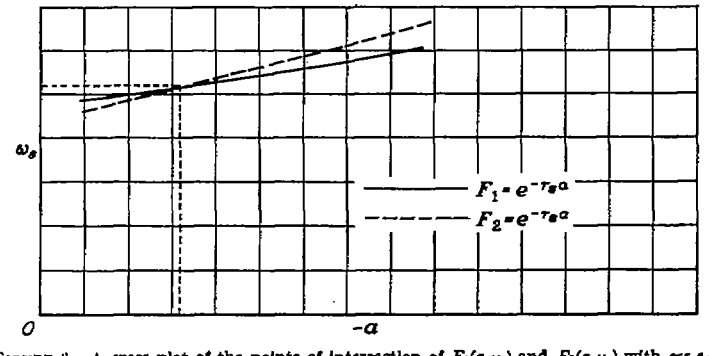

FIGURE 6.—A cross plot of the points of intersection of $F_1(a,\omega_s)$ and $F_2(a,\omega_s)$ with $e^{-\tau_s a}$ as determined from figure 5.

An alternative method for the simultaneous solution of equations (7a) and (7b) is to substitute $1-\tau_s a+\frac{\tau_s^2 a^2}{2}-\frac{\tau_s^3 a^3}{6}$ for $e^{-\tau_s a}$ in each of these equations. The calculations involved become considerably less laborious when this approximation is made and results obtained by using this alternative method have been found to be in excellent agreement with results obtained from the method described previously. Figure 7 shows that for $|\tau_s a|=1$ very close agreement is obtained between the exact value of $e^{-\tau_s a}$ and its approximation by three and four terms of the series for $e^{-\tau_s a}$. In actual practice the product $\tau_s a$ will almost invariably be much less than 1. When this substitution is made, both equations (7a) and (7b) become seventh degree in a for a given value of ω_s. Although these equations are of high degree, no serious problem is presented since the values of a desired must be real and, in general, small; that is, only one or two of the roots of these high-degree equations are of interest. In order to calculate the complex roots of equation (5) for a particular value of τ_s, the following procedure should be used. For a sequence of values of ω_s, compute a from equations (7a) and (7b). The results obtained from each equation may then be plotted in a figure similar to figure 6 and the complex root of the characteristic stability equation determined from the intersection of the two resulting curves. If the value of the approximate series for $e^{-\tau_s a}$ is in good agreement with the exact value of $e^{-\tau_s a}$ for the a determined from the intersection of the two curves, then the complex root obtained is valid. A point of intersection for a value of a which would not give satisfactory agreement between the approximate series and $e^{-\tau_s a}$ might exist, however. If such be the case, the accurate point of intersection is readily ascertained. The estimated values of a and ω_s represent the point of intersection of $F_1(a,\omega_s)$ or $F_2(a,\omega_s)$ with the series approximating $e^{-\tau_s a}$. The desired point is the point of intersection of $F_1(a,\omega_s)$ or $F_2(a,\omega_s)$ with $e^{-\tau_s a}$. The first step is to evaluate the term $e^{-\tau_s a}$ for several values of a in the vicinity of the estimated point of intersection. The expressions $F_1(a,\omega_s)$ and $F_2(a,\omega_s)$ are then evaluated for values of ω_s slightly less than and greater than the estimated value of ω_s for several values of a in the range of the estimated point of intersection. Thus, the corrected curves of equations (7a) and (7b) are obtained and at their point of intersection, the accurate values of a and ω_s are determined.

A method for constructing curves of constant period and damping as a function of τ_s and k_s is presented in the appendix.

Range of ω_s and a to be used in the determination of the complex roots of the characteristic stability equation.—In

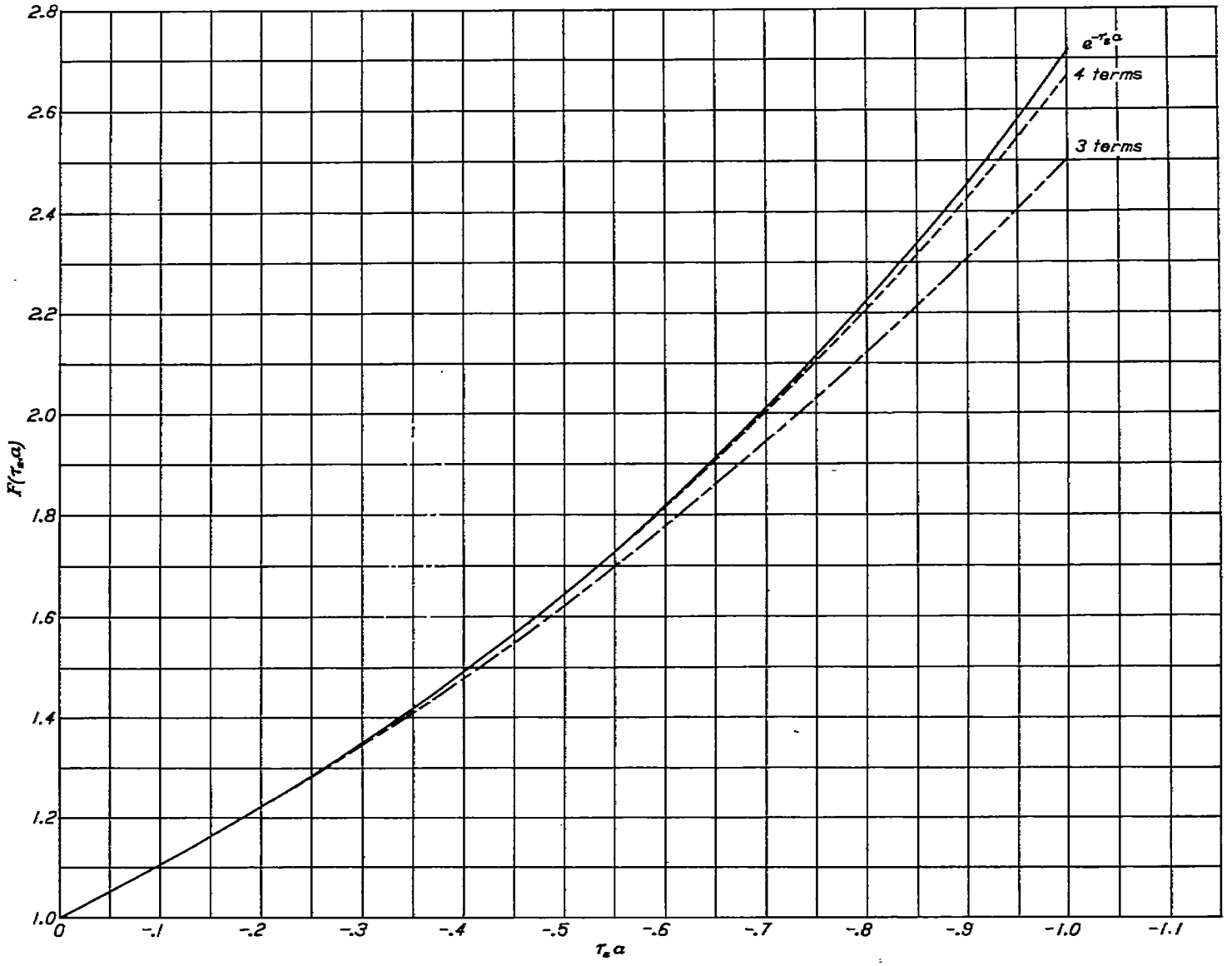

FIGURE 7.—A comparison between $e^{-\tau_s a}$ and its approximation by three and four terms of the series for $e^{-\tau_s a}$.

general, the analysis required to determine the damping of the airplane-autopilot system would be carried out for those values of τ_s that result in a stable system, since the purpose of equipping an airplane with an autopilot is to stabilize or increase the damping of the airplane motions. The range of τ_s for which the system is stable is determined from the frequency-response curves of the airplane and autopilot as indicated in the section entitled "Determination of Critical Time Lag." Thus, if the system is stable, only negative values of a need be investigated. Also, if two stable oscillatory modes of motion exist, the least stable one is of greatest interest—that is, the complex root with the smallest real part is the one of most importance.

The estimated range of values for ω_s that should be used in the analysis to determine the effect of some particular value of time lag, located between $\tau_s=0$ and the critical time lag $(\tau_s)_c$, on the damping of the oscillation is obtained from the known values of the frequency of the oscillation for the cases where $\tau_s=0$ and $\tau_s=(\tau_s)_c$. The imaginary part of the complex root of equation (5), which becomes a quartic equation when $\tau_s=0$, gives the value of ω_s for the case of $\tau_s=0$. The value of ω_s for $\tau_s=(\tau_s)_c$ is determined from the analysis presented in the section entitled "Determination of Critical Time Lag." As mentioned in reference 11, the frequency of the oscillation decreases as time lag increases; thus for a value of $0<\tau_s<(\tau_s)_c$, the estimated values of ω_s should include frequencies greater than the value of ω_s at $\tau_s=(\tau_s)_c$ and less than the value of ω_s at $\tau_s=0$.

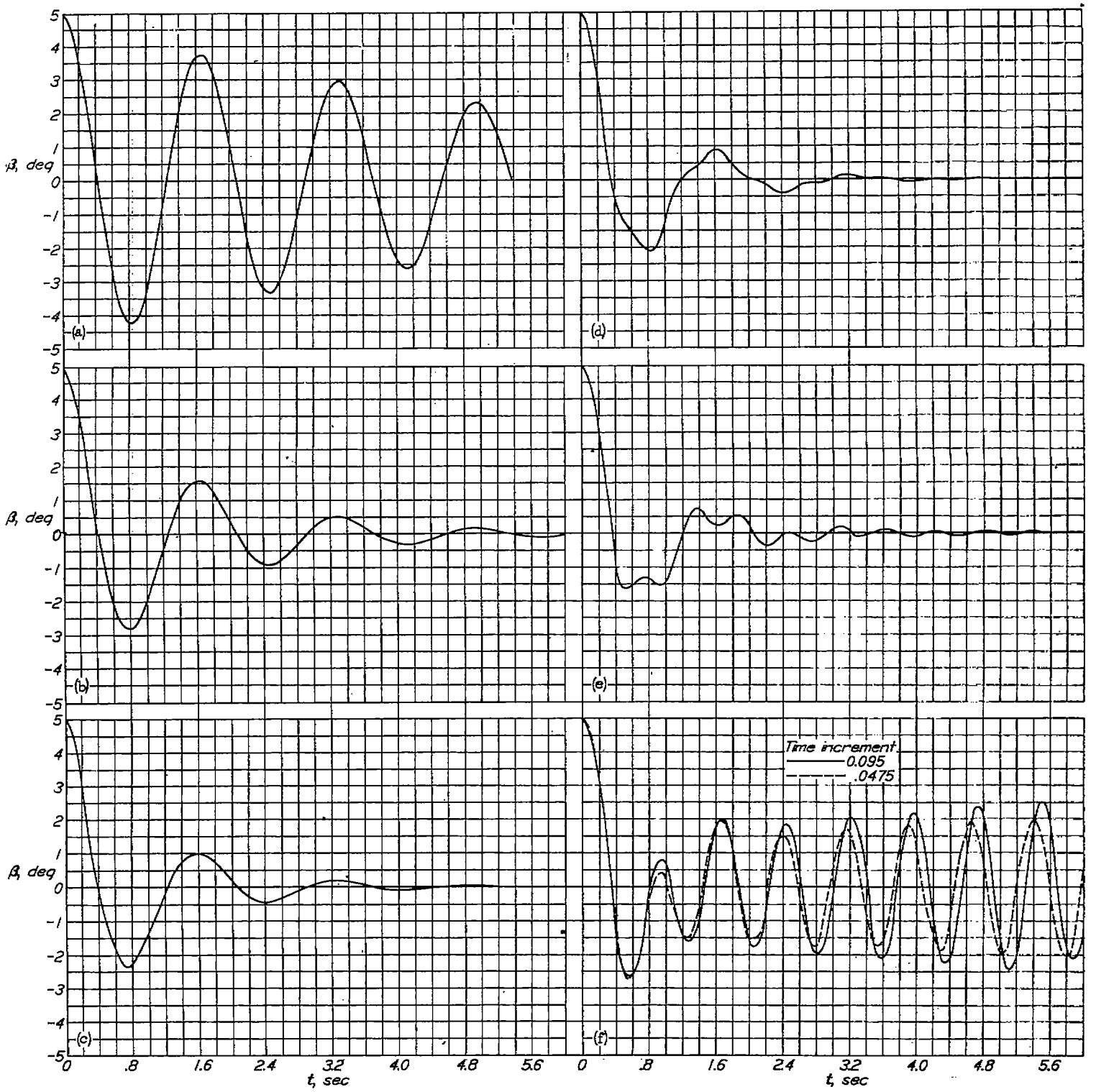

(a) $\tau=0$.
(b) $\tau=0.10$.
(c) $\tau=0.20$.
(d) $\tau=0.25$.
(e) $\tau=0.287$.
(f) $\tau=0.38$ (same as fig. 3).

FIGURE 8.—Effect of time lag on the airplane motion in sideslip.

Airplane motions for various values of τ.—For purposes of comparison, the motion of the airplane in sideslip subsequent to an initial displacement in sideslip of 5° was calculated, with the use of a step-by-step procedure, for τ=0, 0.10, 0.20, 0.25, 0.287, and 0.38. The results are presented in figures 8 (a) to 8 (f). These figures indicate that as τ increases from 0 to 0.2 the period increases slightly, whereas the damping is markedly improved. The frequency of the oscillation is about ω=3.7. However, as τ continues to increase, the presence of a high-frequency oscillation is noted in the motion since this oscillation becomes less damped and the low-frequency oscillation becomes more heavily damped. (See figs. 8 (d) and 8 (e).) For τ=0.38, the motion is neutrally stable at the high frequency of ω=8.5 but the low-frequency oscillation does not appear in this motion since it is very well damped. In figures 9 (a) and 9 (b), the period and damping of the lateral oscillation for several values of τ, calculated by the method discussed in this report, are compared with the period and damping readily obtained from the motion calculations shown in figures 8 (a) to 8 (f). The very good agreement between the results presented in figures 9 (a) and 9 (b) would probably be improved if the increment selected for the step-by-step calculations were reduced. The trends indicated by these results, however, are applicable only to the particular airplane-autopilot system considered in this example and may not be generalized to any other arbitrary airplane-autopilot system.

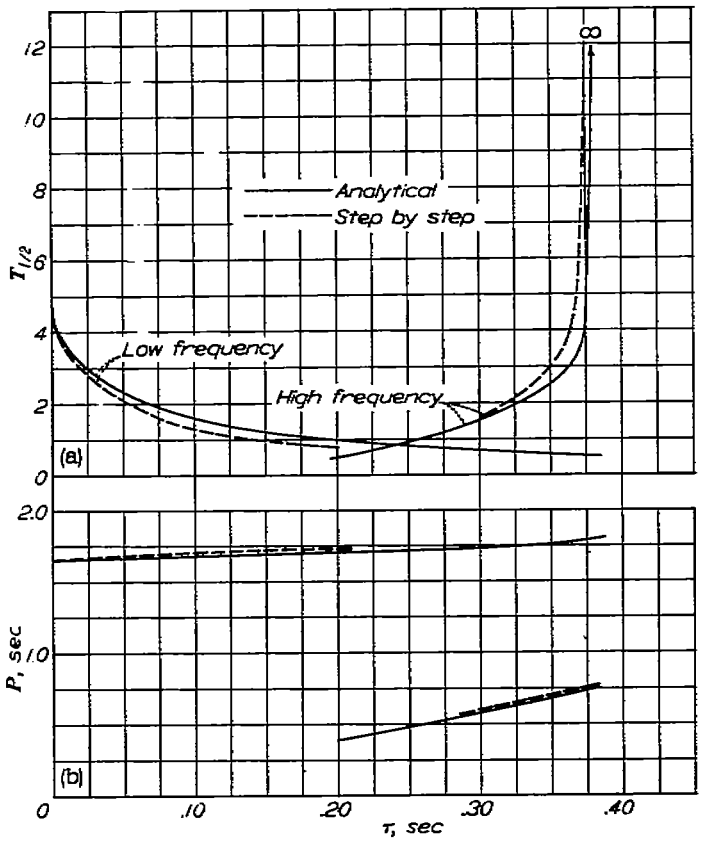

(a) Damping.
(b) Period.

FIGURE 9.—Effect of time lag on the period and damping of the lateral oscillation.

CONCLUDING REMARKS

A method is presented for determining the effect of time lag in an automatic stabilization system on the lateral oscillatory stability of an airplane. The method is applied to a typical present-day airplane equipped with an automatic pilot sensitive to yawing acceleration and geared to the rudder so that rudder control is applied in proportion to the yawing acceleration. The results calculated for an airplane-autopilot system by the method described are in good agreement with the airplane motions calculated by a step-by-step procedure.

LANGLEY AERONAUTICAL LABORATORY,
NATIONAL ADVISORY COMMITTEE FOR AERONAUTICS,
LANGLEY FIELD, VA., *October 28, 1949.*

APPENDIX

A METHOD FOR CONSTRUCTING CURVES OF CONSTANT PERIOD AND DAMPING AS A FUNCTION OF τ_s AND k_s

If an over-all picture is desired of the effect of time lag for a given value of k_s or the effect of varying k_s for a given time lag, construction of curves of constant period and damping with the use of the following method is recommended.

The characteristic stability equation of the airplane-autopilot system (equation (5)) may be rewritten in the form:

$$\frac{A\lambda^4+B\lambda^3+C\lambda^2+D\lambda+E}{-(A'\lambda^4+B'\lambda^3+C'\lambda^2+D'\lambda)}=k_s e^{-\tau_s\lambda} \qquad (A1)$$

If $\lambda=a+i\omega_s$ is substituted in each side of equation (A1), the condition that λ be a root of the characteristic equation is that the complex number A_1+iB_1 obtained from the left-hand side must be equal to the one obtained from the right-hand side A_2+iB_2. The quantities A_1+iB_1 and A_2+iB_2 may be represented by the expressions $R_1e^{i\theta_1}$ and $R_2e^{i\theta_2}$, respectively. Therefore, this requirement is equivalent to saying that $R_1\equiv R_2$ and $\theta_1\equiv\theta_2$ if λ is to be a root of equation (A1). If $\lambda=a+i\omega_s$ is substituted in the right-hand side, the following expressions result:

$$k_s e^{-\tau_s a}(\cos\ \tau_s\omega_s - i\ \sin\ \tau_s\omega_s)=A_2+iB_2=R_2e^{i\theta_2}$$

where

$$R_2=k_s e^{-\tau_s a}$$

and

$$\theta_2=\tan^{-1}\frac{-\sin\ \tau_s\omega_s}{\cos\ \tau_s\omega_s}=-\tau_s\omega_s=2\pi-\tau_s\omega_s$$

Therefore, if $\lambda=a+i\omega_s$ is substituted in the left-hand side and $A_1+iB_1=R_1e^{i\theta_1}$ is obtained, the value of τ required to make $\theta_1=\theta_2$ can be determined. Since τ_s is therefore determined and a is fixed, the value of k_s necessary to make $R_1=R_2$ can be calculated. Thus for these values of k_s and τ_s,

$$\lambda=a+i\omega_s$$

is a root of the transcendental stability equation (equation (5)).

For a given value of a, the analysis may be made throughout the range of ω_s and the corresponding values of k_s and τ_s determined. A curve representing this value of a may then be plotted as a function of k_s and τ_s. This procedure is repeated for a sequence of values of a and the corresponding curves in the k_s,τ_s plane are plotted. Each point on a curve of constant a represents a particular value of ω_s. Curves of constant frequency may therefore be plotted by drawing a curve through the given value of ω_s on each one of the a curves. The values of a and ω_s are converted to $T_{1/2}$ and P by equations (6). The final result would consist of curves of constant damping $T_{1/2}$ and curves of constant period P in the k_s,τ_s plane. Thus the effect of time lag on the lateral oscillations for any value of the gearing ratio k_s, or the effect of varying k_s for any value of time lag, may be ascertained. For purposes of illustration several lines of constant $T_{1/2}$ and P in the k,τ plane were calculated for the typical present-day airplane described in table I and are shown in figure 10.

A curve can be plotted in the k_s,τ_s plane which divides the quadrant into a satisfactory and an unsatisfactory region

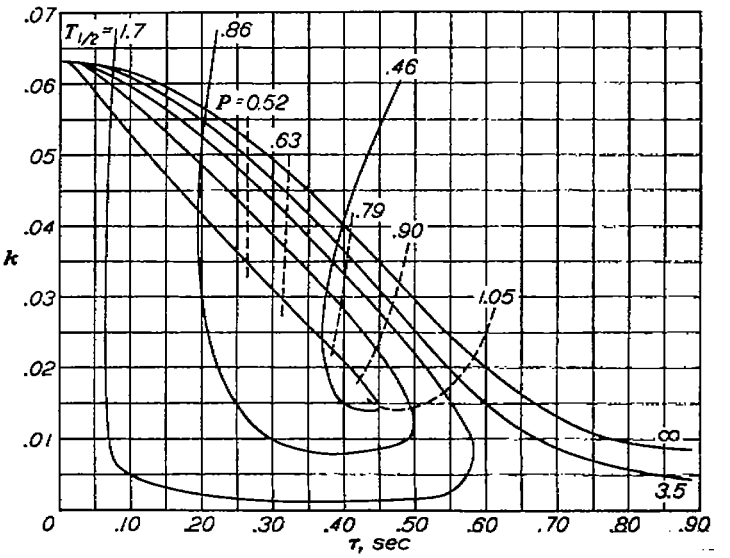

FIGURE 10.—Several curves of constant period and constant damping for the typical present-day airplane described in table I.

according to any prescribed relationship between the period and damping of the lateral oscillation. In order to calculate this curve, several values of a and ω_s that exactly satisfy the criterion should be selected and substituted in equation (A1). The combination of k_s and τ_s is then obtained for each set of values of a and ω_s and the desired curve is plotted in the k_s,τ_s plane.

REFERENCES

1. Sternfield, Leonard: Effect of Automatic Stabilization on the Lateral Oscillatory Stability of a Hypothetical Airplane at Supersonic Speeds. NACA TN 1818, 1949.
2. Imlay, Frederick H.: A Theoretical Study of Lateral Stability with an Automatic Pilot. NACA Rep. 693, 1940.
3. Beckhardt, Arnold R.: A Theoretical Investigation of the Effect on the Lateral Oscillations of an Airplane of an Automatic Control Sensitive to Yawing Accelerations. NACA TN 2006, 1950.
4. Ansoff, H. I.: Stability of Linear Oscillating Systems with Constant Time Lag. Jour. Appl. Mech., vol. 16, no. 2, June 1949, pp. 158–164.
5. Schiff, Leonard I., and Gimprich, Marvin: Automatic Steering of Ships by Proportional Control. Trans. Soc. Naval Arch. and Marine Eng., vol. 57, 1949.
6. Greenberg, Harry: Frequency-Response Method for Determination of Dynamic Stability Characteristics of Airplanes with Automatic Controls. NACA Rep. 882, 1947.
7. Jones, Robert T., and Sternfield, Leonard: A Method for Predicting the Stability in Roll of Automatically Controlled Aircraft Based on the Experimental Determination of the Characteristics of an Automatic Pilot. NACA TN 1901, 1949.
8. Jones, Robert T.: A Simplified Application of the Method of Operators to the Calculation of Disturbed Motions of an Airplane. NACA Rep. 560, 1936.
9. Brown, Gordon S., and Campbell, Donald P.: Principles of Servomechanisms. John Wiley & Sons, Inc., 1948, pp. 170–174.
10. Levy, H., and Baggott, E. A.: Numerical Studies in Differential Equations. Vol. I, Watts & Co. (London), 1934, p. 104.
11. Minorsky, Nicholas: Self-Excited Oscillations in Dynamical Systems Possessing Retarded Actions. Jour. Appl. Mech., vol. 9, no. 2, June 1942, pp. A–65—A–71.